Contribution of Residues in the Reactive Site Loop of Chymotrypsin Inhibitor 2 to Protein Stability and Activity†

Sophie E. Jackson‡ and Alan R. Fersht*

MRC Unit for Protein Function & Design, Cambridge IRC for Protein Engineering, University Chemical Laboratory, Lensfield Road, Cambridge CB2 1EW, U.K.

Received July 15, 1994; Revised Manuscript Received September 8, 1994⊗

ABSTRACT: Residues in the active site loop of the serine protease inhibitor, chymotrypsin inhibitor 2, thought to play an important role in loop stability and inhibitory activity, have been investigated by site-directed mutagenesis. Substitutions at residues 58 (threonine in wild type) and 60 (glutamic acid in wild type), which flank the scissile bond (Met-59-Glu-60) and are conserved among the potato inhibitor I family of serine protease inhibitors, are found to be of some importance in the global stability of the protein, as measured by guanidinium chloride-induced denaturation, but are essential for its inhibitory activity. Mutation of either Thr-58 or Glu-60 to alanine results in a decrease in stability of 0.7 ± 0.1 kcal mol^{-1}. These values reflect the loss of hydrogen bonds between the hydroxyl group of Thr-58 with Glu-60 and Arg-67 and hydrogen bonds and a salt bridge between Glu-60 and Arg-62 and Arg-65. In addition, these mutants were found to be much weaker inhibitors of the serine protease subtilisin BPN′. The dissociation constants for inhibition, K_i, were found to be (7.0 ± 0.4, 540 ± 30, and 980 ± 50) × 10^{-13} M, for wild type, T58A, and E60A, respectively. Further, we find that these mutants are only temporary inhibitors of subtilisin BPN′, unlike wild type. Over long time scales, we observe a reversal of inhibition because of hydrolysis of the inhibitor. In addition, we have found from double-mutant cycle analysis on T58AE60A and T58DE60A that there are interaction energies between residues 58 and 60 in the free inhibitor of 0.5 ± 0.2 and 0.4 ± 0.1 kcal mol^{-1} (measured for T58AE60A and T58DE60A, respectively) that increase substantially in the complex with subtilisin BPN′ to 2.1 ± 0.1 and 4.2 ± 0.2 kcal mol^{-1}, respectively. The hydrogen bonding and salt bridge network within the active site loop, which is a characteristic of potato inhibitor I family of inhibitors, is essential for the inhibitory activity of the protein.

Serine proteases are common in nature and have a wide variety of biological roles, including digestion of proteins for nutrition, generation of active hormones, control of blood clotting, fertilization, and transport of secretory proteins across membranes (Neurath, 1984). Modulation of protease activity is consequently of some importance. Inhibitors of serine proteases exist in animal, plant, and microbial organisms with the physiological function of preventing unwanted proteolysis. Serine protease inhibitors act as competitive inhibitors by binding tightly to the active site of the protease. Dissociation constants are typically 10^{-8}−10^{-16} M (Laskowski & Kato, 1980). Despite much research in this area, it is still not clear what structural features are essential for their functioning as inhibitors and prevent them from being well-designed substrates. To investigate further the structural basis for inhibition, we have performed site-directed mutagenesis on residues in the reactive site loop of chymotrypsin inhibitor 2. Chymotrypsin inhibitor 2, CI2, is a member of the potato inhibitor I family of serine protease inhibitors (Jonassen, 1980). It is found naturally in the albumin fraction of seeds from the *Hiproly* strain of barley. CI2 is a potent inhibitor of subtilisin BPN′, with a K_i in the picomolar range. It inhibits chymotrypsin and elastase some 500- and 10 000-fold weaker, respectively, and does not inhibit and is hydrolysed by trypsin (Longstaff et al., 1990). A truncated, 64-residue, form of the protein, lacking the first, unstructured, 19 amino acids, is used in these studies (Jackson et al., 1993a). It is a single domain protein whose tertiary structure consists of a central four-stranded mixed parallel and antiparallel β-sheet which is packed against an α-helix to form the hydrophobic core (McPhalen & James, 1987). Between parallel strands 2 and 3, on the opposite side of the β-sheet to the α-helix, is a wide loop in extended conformation which contains the reactive site bond, Met-59-Glu-60; see Figure 1. Unlike many other serine protease inhibitors, CI2 contains no disulfide bonds. Inhibitors from other families have disulfide bonds which flank the reactive site bond and which stabilize the reactive site loop. Although these are not present in the potato inhibitor I family, CI2 appears to have some comparable noncovalent interactions. Two highly conserved arginine residues, Arg-65 and Arg-67, stabilize the reactive site loop through hydrogen-bonding and electrostatic interactions with Thr-58 and Glu-60; see Figure 1 and Table 1. Evidence from other studies on chymotrypsin inhibitor 1 (Boisen et al., 1981) and eglin c (Heinz et al., 1992) suggests that the stability of the reactive site loop is a key element in their ability to inhibit serine proteases.

In this paper, we present a comprehensive study on five CI2 mutants containing point mutations in the reactive site loop. Substitutions were made at positions 58 (Thr in wild

† S.E.J. is a William Stone Research Fellow, Peterhouse, Cambridge.

* Author to whom correspondence should be addressed.

‡ Present address: Department of Chemistry, Harvard University, 12 Oxford Street, Cambridge, MA 02138.

⊗ Abstract published in *Advance ACS Abstracts,* October 15, 1994.

0006-2960/94/0433-13880$04.50/0

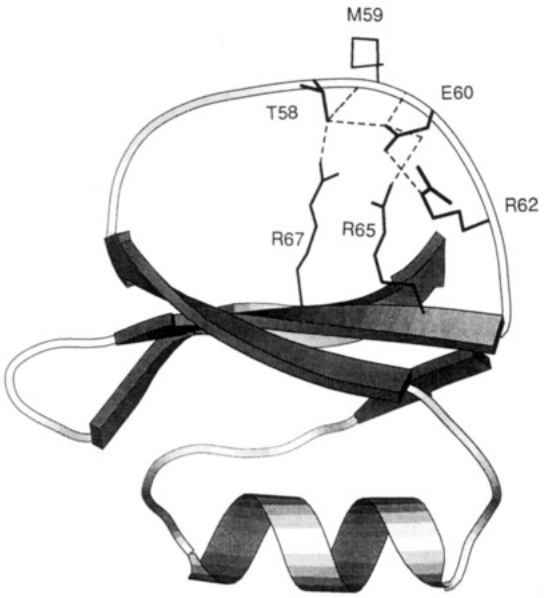

FIGURE 1: Secondary and tertiary structure of chymotrypsin inhibitor 2. Residues in the reactive site loop are shown. Possible hydrogen bonds and salt bridges between these residues are indicated by the dashed lines. The diagram was produced using the program *MolScript* (Kraulis, 1991).

Table 1: Putative Hydrogen Bonding Groups in the Reactive Site Loop of Chymotrypsin Inhibitor 2[a]

residue	group	partner	distance (Å) (donor/acceptor)
Thr-58	$O^{\gamma 1}$	$O^{\epsilon 2}$ Glu-60	2.8
	$O^{\gamma 1}$	$N^{\eta 2}$ Arg-67	2.7
Glu-60	$O^{\epsilon 2}$	N Glu-60	2.7
	$O^{\epsilon 1}$	N^{ϵ} Arg-62	2.9
	O	$N^{\eta 2}$ Arg-65	2.9
Arg-62	N	$O^{\tau 1}$ Gly83[b]	2.9
Arg-65	$N^{\eta 2}$	$O^{\tau 1}$ Gly83[b]	2.8
Arg-65	N^{ϵ}	$O^{\tau 2}$ Gly83[c]	2.7

[a] Calculated from the structure of chymotrypsin inhibitor 2 complexed to subtilisin BPN′ (McPhalen et al., 1985). The crystal structure of the free inhibitor (McPhalen & James, 1987) is not used because the structure of the reactive site loop is very poorly defined. Average B-factors for Thr-58, Met-59, and Glu-60 are 43, 47, and 36 Å^2 in the free inhibitor and 7, 11, and 8 Å^2 in the structure of the complex, respectively. The structure of the reactive site loop is also poorly defined in the nuclear magnetic resonance solution structure (Ludvigsen et al., 1991). This results from its extended conformation reducing the number of long-range NOEs available to constrain the structure. We, therefore, use the structure of the complex as a guide to the possible hydrogen-bonding and salt bridges in the reactive site loop. [b] Gly83 is the carboxy-terminal residue, $O^{\tau 1}$ is used to denote one of the oxygens of the carboxy terminus. [c] $O^{\tau 2}$ is used to denote the other oxygen of the carboxy terminus.

type) and 60 (Glu in wild type), which disrupt the hydrogen-bonding and salt bridge network within the reactive site loop. The functional properties of these mutants were studied using presteady state inhibition kinetics of the slow, tight-binding inhibition of the serine protease subtilisin BPN′ (cf. Longstaff et al., 1990). In addition, the effect of the mutations on the stability of the protein was investigated using guanidinium chloride denaturation (cf. Jackson & Fersht, 1991a,b; Jackson et al., 1993a,b) to measure the contribution that Thr-58 and Glu-60 make to both protein stability and activity and to investigate the relationship between them. Further, two double mutants at these positions were constructed, which have yielded information on the interactions between these residues in the native state, in both the free inhibitor and in complex with subtilisin BPN'. These data give insights into the mechanism of inhibition of this class of serine protease inhibitor.

EXPERIMENTAL PROCEDURES

Materials

Chemicals. The buffer used in denaturation experiments was 2-(*N*-morpholino)ethanesulfonic acid (MES) purchased from Sigma. Succinyl-Ala-Ala-Pro-Phe-*p*-nitroaniline, sAAPFpNA, was prepared as a stock solution in dimethyl sulfoxide, DMSO, which had been dried over barium oxide and distilled under vacuum. Guanidinium chloride was sequanal grade purchased from Pierce Chemicals. Water was purified to 15 MΩ resistance by an Elgastat system. Radiochemicals were from Amersham International. DEAE trisacryl was obtained from IBF, Villeneuve La Garenne, France. Yeast extract and tryptone were purchased from Lab M, Bury, U.K. Ammonium sulfate was enzyme grade from BDH. All other chemicals were purchased from Sigma.

Mutagenesis. Single-stranded DNA was obtained from the modified pTZ18U, harbored in *E. coli* TG2 after infection with the helper phage M13KO7 following the conditions described by Pharmacia. Site-directed mutagenesis was carried out using the method of Eckstein (Sayers et al., 1988) and the kit supplied by Amersham (using 0.2 of the recommended amounts of DNA and kit). Mutants were identified by directly sequencing the single-stranded DNA. Wild type and mutants were expressed and purified (Jackson et al., 1993a).

Methods

Chemical denaturation experiments were performed exactly as described by Jackson et al. (1993a) and the data analyzed by fitting to the equation

$$F = [(\alpha_N + \beta_N[\mathrm{GdnHCl}]) + ((\alpha_U + \beta_U[\mathrm{GdnHCl}]) \exp(m([\mathrm{GdnHCl}] - [\mathrm{GdnHCl}]_{50\%})))/RT]/ [1 + \exp(m([\mathrm{GdnHCl}] - [\mathrm{GdnHCl}]_{50\%}))/RT] \quad (1)$$

where F is the observed fluorescence, α_N and α_U are the intercepts, and β_N and β_U are the slopes of the base lines at the low (N) and high (U) guanidinium chloride concentrations, $[\mathrm{GdnHCl}]_{50\%}$, the concentration of guanidinium chloride at which 50% of the protein is denatured, m is a constant that is proportional to the increase in degree of exposure of the protein on denaturation, and R is the gas constant, 8.314 J mol^{-1} K^{-1}. $\Delta G_{U-F}^{H_2O}$, the free energy of unfolding in water, $\Delta\Delta G_{U-F}^{[\mathrm{GdnHCl}]50\%}$, the difference in stability between wild-type and mutant protein at a concentration [GdnHCl] = 0.5($[\mathrm{GdnHCl}]_{50\%} - [\mathrm{GdnHCl}]'_{50\%}$), where $[\mathrm{GdnHCl}]'_{50\%}$ is the midpoint of unfolding of mutant, and $\Delta\Delta G_{U-F}^{H_2O}$, the difference in stability between wild-type and mutant protein in water, can be calculated from this data. Equations and a comparison of the different methods has been discussed in detail elsewhere (Jackson et al., 1993a).

Slow-Binding Inhibition Kinetics. Chymotrypsin inhibitor 2 can be treated as a slow, tight-binding inhibitor of subtilisin BPN′ (Longstaff et al., 1990). General experimental procedures, and the methods for determining k_{on}, the association rate constant, k_{off}, the dissociation rate constant, and K_i, the dissociation constant for the enzyme−inhibitor complex,

Table 2: Changes in the Free Energies of Unfolding upon Mutation Determined by Reversible Guanidinium Chloride Denaturation Experiments

mutant	$[GdnHCl]_{50\%}$[a] (M)	m[a] (kcal mol^{-2})	$\Delta G_{U-F}^{H_2O}$ [b] (kcal mol^{-1})	$\Delta\Delta G_{U-F}^{H_2O}$ [b] (kcal mol^{-1})	$\Delta\Delta G_{U-F}^{[GdnHCl]50\%}$ [b] (kcal mol^{-1})
wild-type[c]	3.99 ± 0.02	1.89 ± 0.04	7.53 ± 0.16		
T58D	4.01 ± 0.03	1.87 ± 0.08	7.50 ± 0.33	0.04 ± 0.36	−0.04 ± 0.07
T58A	3.63 ± 0.04	1.89 ± 0.14	6.86 ± 0.51	0.68 ± 0.54	0.69 ± 0.09
E60A	3.64 ± 0.05	1.78 ± 0.16	6.48 ± 0.59	1.06 ± 0.61	0.68 ± 0.11
T58AE60A	3.54 ± 0.02	1.94 ± 0.10	6.87 ± 0.36	0.67 ± 0.39	0.87 ± 0.07
T58DE60A	3.86 ± 0.02	1.89 ± 0.09	7.30 ± 0.35	0.24 ± 0.38	0.25 ± 0.06

[a] Calculated from direct fit of data to eq 1. [b] For method of calculation see Jackson et al. (1993a). [c] Average of four separate experiments. Errors given are standard errors.

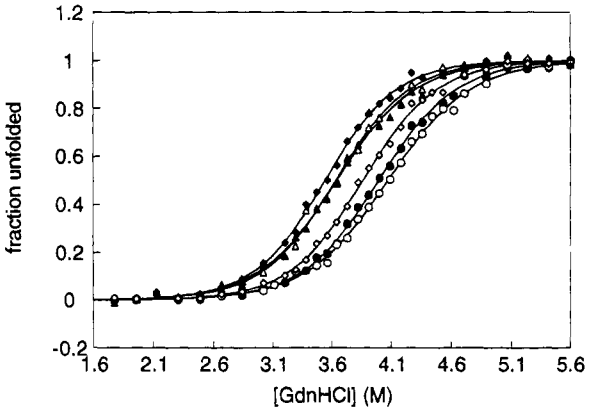

FIGURE 2: Guanidinium chloride-induced equilibrium unfolding of wild-type and mutant chymotrypsin inhibitor 2: (●) wild-type, (○) T58D, (▲) E60A, (△) T58A, (◆) T58AE60A, (◇) T58DE60A. Unfolding was monitored by the intrinsic fluorescence of CI2 using an excitation wavelength of 280 nm and an emission wavelength of 356 nm. Under these conditions the base lines of the native and denatured state are found to be dependent upon [GdnHCl]. These plots show the data normalized (fraction unfolded) taking into account the sloping base lines. The solid lines are the best fit of the data to a two-state process.

have been described elsewhere (Jackson & Fersht, 1993; Cha, 1975; Williams & Morrison, 1979).

In the experiments described in this paper the experimental conditions were as follows. The range of inhibitor concentrations used depended on the dissociation constant, typically 1−5 nM for wild type, T58A, T58D, and T58DE60A and 3−12 nM for E60A and T58AE60A, while the enzyme concentration was typically 5 pM. The substrate concentration was typically 0.6 mM. A Cary 3 UV−vis spectrophotometer with an automatic cell changer (2 × six cells)was used. Data were collected using the applications software package (Software Issue 2.00, Instrument Software Issue 3.00) provided by Cary for 7−8 h. The data were translated into ASCII format using the Cary data import/export program (Varian Associates (1990) Release 3.00) and then analyzed using the nonlinear regression analysis program *Kaleidagraph* as previously described (Jackson & Fersht, 1993; Cha, 1975; Williams & Morrison, 1979).

RESULTS

Stability Studies

GdnHCl-Induced Denaturation. Wild type and mutants were found to follow two-state unfolding transitions. Typical normalized GdnHCl-induced denaturation curves are shown in Figure 2. Data from such transition curves were fitted to eq 1 to yield values for $[GdnHCl]_{50\%}$ and m for each mutant and associated errors. These values can then be used to calculate $\Delta G_{U-F}^{H_2O}$, $\Delta\Delta G_{U-F}^{[GdnHCl]50\%}$, and $\Delta\Delta G_{U-F}^{H_2O}$. These results are shown in Table 2. It is clear that the errors associated with $\Delta\Delta G_{U-F}^{H_2O}$ are substantially larger than those in calculating $\Delta\Delta G_{U-F}^{[GdnHCl]50\%}$, as has been previously reported (Jackson et al., 1993a). $\Delta\Delta G_{U-F}^{[GdnHCl]50\%}$ is used in the subsequent analysis.

Double Mutant Cycle Analysis of T58AE60A and T58DE60A. Double mutant cycles can be used to measure the interaction energy, $\Delta\Delta G_{int(F)}$, between two residues in the folded state of a protein. $\Delta\Delta G_{int(F)}$ can be calculated according to the general equation below

$$\Delta\Delta G_{int(F)} = \Delta G_{U-F}^{E-XY\rightarrow EX} - \Delta G_{U-F}^{E-Y\rightarrow E} = \Delta G_{U-F}^{E-XY\rightarrow EY} - \Delta G_{U-F}^{E-X\rightarrow E} \quad (2)$$

where E stands for the protein, X and Y the two residues being mutated, and $\Delta G_{U-F}^{E-XY\rightarrow EX}$, $\Delta G_{U-F}^{E-Y\rightarrow E}$, $\Delta G_{U-F}^{E-XY\rightarrow EY}$, $\Delta G_{U-F}^{E-X\rightarrow E}$ for the free energy changes for the appropriate transitions in the cycle. Each of the free energy terms on the right-hand side of the equation is determined by measuring the difference in the free energy of the initial and final states of the respective transition. Thus, for example, $\Delta G_{U-F}^{E-XY\rightarrow EX}$ is the difference in unfolding free energies between E−XY and E−X (Horovitz & Fersht, 1990; Horovitz et al., 1990).

The interaction energy between Thr-58 and Glu-60 is 0.50 ± 0.16 kcal mol^{-1} and between Asp-58 and Glu-60 is 0.39 ± 0.14 kcal mol^{-1}, in the native state of the protein. Thus, there is a significant interaction energy between Thr-58 or Asp-58 and Glu-60. The positive sign indicates that, in both cases, the double mutant is less destabilizing than expected from the sum of the single mutants.

Activity Studies

Case 1: Classical Slow Tight-Binding Inhibition Kinetics. Wild type, T58D, and T58DE60A behave as classical slow, tight-binding inhibitors of subtilisin BPN′. A typical set of binding curves is shown in Figure 3a. Data from these curves were fitted to give values for k_{obs}, the apparent first-order rate constant for the transition to the steady-state rate, v_s, the final steady-state rate, and v_o, the initial rate, at each inhibitor concentration. Plots of k_{obs} *versus* inhibitor concentration were used to calculate the association rate, k_{on}, for the binding of inhibitor to subtilisin BPN′ (Jackson & Fersht, 1993). A typical plot is shown in Figure 4a. These plots were linear over the inhibitor concentration range studied. Values for k_{on} are given in Table 3. With the exception of T58D, the values of k_{on} for the mutants are very

Table 3: Parameters from Slow, Tight-Binding Kinetic Analysis of Wild-Type and Mutant CI2

mutant	k_{on} ($\times 10^6$ M^{-1} s^{-1})	k_{off} ($\times 10^{-6}$ s^{-1})	K_i ($\times 10^{-13}$ M)	K_i^{mut}/K_i^{wt}	$\Delta\Delta G_{binding}$ (kcal mol^{-1})	k_d (s^{-1})
wild-type	5.5 ± 0.4	3.9 ± 0.3	7.0 ± 0.4	1	0	
T58D	1.4 ± 0.1	34 ± 3	242 ± 14	43	2.06 ± 0.10	*a*
T58A	3.8 ± 0.4	206 ± 25	538 ± 31	77	2.57 ± 0.08	
E60A			975 ± 48	139	2.92 ± 0.07	1.6×10^{-4}
T58AE60A			2140 ± 120	306	3.39 ± 0.08	3.5×10^{-4}
T58DE60A	4.3 ± 0.2	10.7 ± 0.1	25 ± 2	3.6	0.75 ± 0.10	
V70A	4.6 ± 0.3	3.4 ± 0.3	7.3 ± 0.4	1.04	0.02 ± 0.04	

[a] Not determined. Although T58A shows some signs of reversal of inhibition over long time scales it was not significant enough for an accurate determination of k_d.

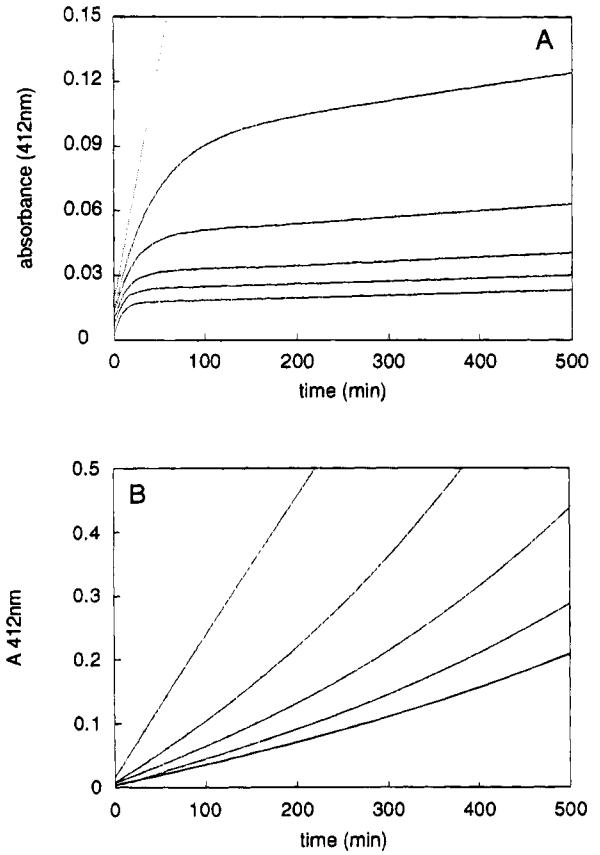

FIGURE 3: Typical families of binding curves for the inhibition of subtilisin BPN′ by wild-type and mutant chymotrypsin inhibitor 2. (A) Classical slow, tight-binding inhibition kinetics shown by wild-type, T58A, T58D, and T58DE60A. (B) Reversal of inhibition caused by destruction of inhibitor shown by E60A and T58AE60A.

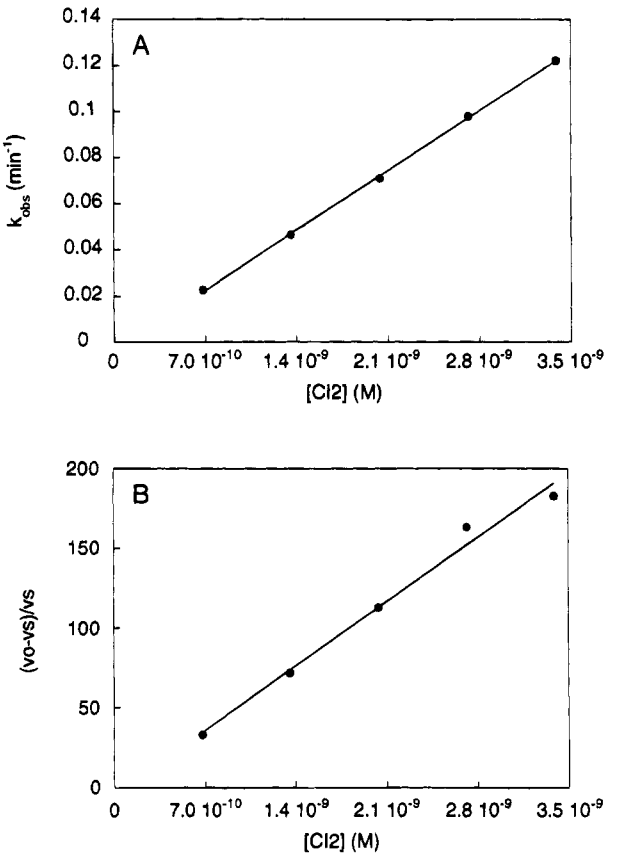

FIGURE 4: Typical plots for the determination of k_{on} and K_i from binding curves. (A) Plot of k_{obs} *versus* inhibitor concentration. From the slope and intercept on the y axis, values for k_{on} and k_{off} can be determined, respectively (Jackson & Fersht, 1993). (B) Plot of $(v_o - v_s)/v_s$ *versus* inhibitor concentration. K_i can be determined from the slope of the plot (Jackson & Fersht, 1993).

similar to that of wild type. The value of k_{on} for T58D is significantly lower than this and could possibly result from conformational changes required on binding of this mutant to subtilisin BPN′. Theoretically, the dissociation rate, k_{off}, can also be determined from the intercept on the y axis of such a plot. In this case, however, the intercept is so close to zero that an accurate value for k_{off} cannot be measured.

K_i was determined from plots of $(v_o - v_s)/v_s$ *versus* inhibitor concentration (Jackson & Fersht, 1993). A typical plot is shown in Figure 4b. It is linear and passes through the origin. For slow-binding inhibitors, equilibrium is reached slowly and it is important to run the experiments for sufficient time so that a good estimate of v_s can be obtained from fitting. In this case, experiments were run for 7 −8 h. If the experiment is not run for sufficient time, then systematic errors can be generated that can be misinterpreted as unusual binding. This is readily diagnosed in plots such as those shown in Figure 4b, which become nonlinear in these cases. All the plots of $(v_o - v_s)/v_s$ *versus* inhibitor concentration were found to be linear. The results are summarized in Table 3.

The plots of k_{obs} *versus* inhibitor concentration are linear. Thus, the kinetic data are consistent with a reaction, eq 3, in which enzyme and inhibitor combine to form the final complex.

$$E + I \underset{k_{off}}{\overset{k_{on}}{\rightleftharpoons}} EI \qquad (3)$$

Values for k_{off} can, therefore, be determined indirectly from measurements of k_{on} and K_i ($k_{off} = k_{on}K_i$). The results are shown in Table 3. T58A also behaves as a slow, tight-binding inhibitor over short time scales (0−300 min), and data were treated as above. Over longer time scales (0−500 min), however, then some reversal of inhibition is observed; see the next section.

Case 2: Reversal of Inhibition by Destruction of Inhibitor. E60A and T58AE60A are much weaker inhibitors of subtilisin BPN′ than wild-type CI2. Therefore, the concentration range of inhibitor used was higher than for wild type. Consequently, the association rate (k_{on}[CI2]) is higher and slow-binding of the inhibitor to subtilisin BPN′ is not observed; i.e., a steady-state is achieved within the dead-time of the experiment. More importantly, E60A and T58AE60A both exhibit temporary inhibition. Over long time scales there is a reversal of inhibition due to the slow destruction of the inhibitor. In this case, this is probably due to the slow hydrolysis of the reactive site bond by subtilisin BPN′. This results in an upward curvature of the binding curves as shown in Figure 3b. Curvature is most significant at low concentrations of inhibitor. Although data cannot be fitted to the slow, tight-binding equation, K_i can still be determined from the binding curves by taking the slope at $t = 0$ as v_s and the rate of the uninhibited enzyme as v_o. K_i may then be calculated as before. Plots of $(v_o - v_s)/v_s$ *versus* inhibitor concentration are linear and pass through the origin. Results are shown in Table 3.

The two mutants, E60A and T58AE60A, which show noticeable reversal of inhibition are also the two most destabilized mutants; see Table 2. The fraction of unfolded protein for these is higher than for wild type or the other mutants. To ensure that hydrolysis is not occurring on the unfolded form of the protein, we perfomed a slow, tight-binding assay on a destabilized mutant in the hydrophobic core of the protein. V70A destabilizes the protein by 1.95 kcal mol^{-1} (Jackson et al., 1993a). This mutant shows perfect slow, tight-binding inhibition kinetics and no reversal of inhibition due to depletion of inhibitor. The value of K_i is within experimental error of the wild-type value. Thus, the reversal of inhibition is not due to the global destabilization of the protein but must be due to a local destabilization of the reactive site loop.

Calculation of the Rate of the Destruction of Inhibitor by Subtilisin BPN′. The following reaction scheme is assumed in which inhibitor reacts rapidly with the enzyme whose inhibition is being measured and then is more slowly destroyed (reaction scheme I):

$$E + I \overset{K_i}{\rightleftharpoons} EI \overset{K_i^*}{\rightleftharpoons} EI^* \underset{k_{-2}}{\overset{k_2}{\rightleftharpoons}} E + I^*$$

where EI is the enzyme−inhibitor complex, EI* is the enzyme−inhibitor complex in which the reactive site bond has been hydrolyzed, I* is the hydrolyzed inhibitor product, K_i^* is the equilibrium constant for nonhydrolyzed and hydrolyzed enzyme-bound inhibitor, and k_2 and k_{-2} are the dissociation and association rate constants for the enzyme−hydrolyzed inhibitor complex, respectively. This can be simplified to reaction scheme II:

$$E + I \overset{K_i}{\rightleftharpoons} EI \overset{k_d}{\longrightarrow} E + I^*$$

Data from binding curves were converted from absorbance at 412 nm into fractional inhibition, i, and then fitted to eq 4 (Goldstein, 1944)

$$\frac{1}{i_o} + \ln\left(\frac{i_o}{1 - i_o}\right) - \frac{1}{i} + \ln\left(\frac{i}{1 - i}\right) = k_d E_I' t \qquad (4)$$

where i_o is the fractional inhibition at $t = 0$, i is the fractional inhibition at time t, k_d is as above, and $E_I' = E_{total}/K_i$. Values of k_d calculated for E60A and T58AE60A are shown in Table 3. Although T58A does show some reversal of inhibition, it is not significant enough for an accurate determination of k_d.

Binding Energies. Dissociation constants may be converted into binding energies using eq 5

$$\Delta\Delta G_{binding} = -RT \ln(K_i/K_i') \qquad (5)$$

where $\Delta\Delta G_{binding}$ is the difference in the binding energy of wild-type and mutant inhibitor to subtilisin BPN′, K_i is the dissociation constant for wild-type CI2, and K_i' is the dissociation constant for mutant CI2. Values of $\Delta\Delta G_{binding}$ for all mutants are shown in Table 3.

Double Mutant Cycle Analysis of T58AE60A and T58DE60A in the Complex with Subtilisin BPN′. Double mutant cycles can also be used to measure the interaction energy, $\Delta\Delta G_{int(EI)}$, between residues 58 and 60 in the complex formed between CI2 and subtilisin BPN′, in a manner analogous to that described for $\Delta\Delta G_{int(F)}$:

$$\begin{aligned}\Delta\Delta G_{int(EI)} &= \Delta G_{binding}^{E-XY \rightarrow EX} - \Delta G_{binding}^{E-Y \rightarrow E} \\ &= \Delta G_{binding}^{E-XY \rightarrow EY} - \Delta G_{binding}^{E-X \rightarrow E}\end{aligned} \qquad (6)$$

By using the binding energies given in Table 3 for the single and double mutants, $\Delta\Delta G_{int(EI)}$ for T58AE60A is 2.10 ± 0.13 kcal mol^{-1} and for T58DE60A $\Delta\Delta G_{int(EI)}$ is 4.23 ± 0.16 kcal mol^{-1}.

DISCUSSION

Contribution of Residues in the Reactive Site Loop to Protein Stability. Thr-58 and Glu-60 both contribute some 0.7 kcal mol^{-1} to protein stability (Table 2). Threonine at position 58 and an acidic residue at position 60 are highly conserved within the potato inhibitor I family of serine protease inhibitors; see Table 4. Mutation of Thr-58 to Ala could result in the loss of two possible hydrogen bonds between $O^{\gamma 1}$ of Thr-58 and $O^{\epsilon 2}$ of Glu-60, and $N^{\eta 2}$ of Arg 67, see Table 1, and van der Waals interactions of C^{γ}. In this case, the side chain is exposed to solvent and C^{γ} makes no van der Waals contacts; therefore, the destabilization energy reflects the loss of hydrogen bonds. Studies on the tyrosyl-tRNA synthetase (Fersht et al., 1985), barnase (Serrano et al., 1992), and T4 lysozyme (Alber et al., 1987; Alber, 1989) have shown that the destabilization energy on deletion of a hydrogen-bonding group from a protein is highly variable and context-dependent. For deletion of a side-chain group that makes a hydrogen bond with a charged group in which there is access of water to the site of mutation, $\Delta\Delta G_{U-F}$ is found to vary between 0 and 1.9 kcal mol^{-1}. The destabilization energy measured for T58A is consistent with these values.

The mutation T58D creates a possible salt bridge with Arg-67. Single, solvent-exposed salt bridges have been found to contribute between 0.3 and 1 kcal mol^{-1} to protein stability (Akke & Forsén, 1990; Dao-Pin et al., 1991; Horovitz et al., 1990; Sali et al., 1991). In this case, however, a favorable electrostatic interaction with Arg-67 is likely to be offset by (i) the loss of the hydrogen bond with Glu-60 and (ii) an unfavorable electrostatic interaction with Glu-60. These

Table 4: Homologies in the Reactive Site Loop between Chymotrypsin Inhibitor 2 and Other Potato Inhibitor I Family Serine Protease Inhibitors[a]

protein	residue no.							
	57	58	59	60	61	62	65	67
CI2	V	T	M	E	Y	R	R	R
CI2 A (barley)	V	T	M	E	Y	R	R	R
CI2 B fragment (barley)	V	T	M	E	Y	R	R	R
CI1 C (barley)	V	P	L	N	F	N	R	F
CI1 A (barley)	V	H	L	N	F	D	R	F
CI1 B (barley)	V	P	L	D	F	N	R	F
subtilisin inhibitor (broad bean)	V	T	A	D	Y	K	R	R
wound-induced PI1 precursor (peruvian tomato)	V	T	K	D	F	R	R	R
subtilisin inhibitor I & II (adzuki beans)	V	T	A	D	Y	N	R	R
wound-induced PI1 precursor (potato)	F	T	E	D	L	R	R	R
ethylene responsive PI1 precursor (potato)	F	T	E	D	L	R	R	R
CI1 A, B, and C subunits (potato)	V	T	M	D	F	R	R	R
wound-induced PI1 precursor (tomato)	I	T	L	D	F	L	R	R
trypsin and Hageman factor inhibitor (pumpkin)	V	T	K	D	L	R	R	R
eglin c (leech)	V	T	A	D	Y	R	R	R

[a] Calculated using homology-derived secondary structure of proteins program (Sander & Schneider, 1991).

unfavorable and favorable interactions balance out which results in the mutation having little, or no, effect on protein stability.

The mutation E60A removes three possible hydrogen bonds between $O^{\epsilon 1}$ and N^{ϵ} of Arg-62, $O^{\epsilon 2}$ and the hydroxyl group of Thr-58, and $O^{\epsilon 2}$ and the NH of its own backbone, see Table 1. In addition, the mutation may remove an exposed salt bridge with Arg-65. Removal of this group and these favorable interactions may be offset by the access of water to the point of mutation replacing some of the lost hydrogen bonds. The mutant is, therefore, only destabilized by 0.7 kcal mol^{-1}.

The double mutant T58AE60A, in which two of the groups involved in the hydrogen-bonding and salt bridge network in the active site loop are lost, is the most destabilized. T58AE60A, however, is only slightly destabilizing. This suggests that an aspartic acid group at position 58 can replace some of the interactions lost on deletion of the glutamic acid group at position 60.

Interaction between Thr-58/Asp-58 and Glu-60 in Free Inhibitor. The interaction energy between a threonine or aspartic acid at position 58 and glutamic acid at position 60 can be calculated using double mutant cycles. A formal analysis of the use of double mutant cycles to calculate interaction energies is given elsewhere (Horovitz & Fersht, 1990; Horovitz et al., 1990) and will not be discussed in detail here. We find there is a significant interaction energy for both double mutants. $\Delta\Delta G_{int(F)} = 0.50 \pm 0.16$ and 0.39 ± 0.14 kcal mol^{-1}, for T58AE60A and T58DE60A, respectively. For T58AE60A, the interaction energy results from the hydrogen bond between the hydroxyl group of Thr-58 and the $O^{\epsilon 2}$ of Glu-60, which is lost on mutation of either T58A or E60A. Thus, this hydrogen bond contributes, in effect, some 0.4 kcal mol^{-1} to protein stability. For T58DE60A, the introduction of the aspartic acid group at position 58 in the presence of the glutamic acid at position 60 (T58D mutant) may result in unfavorable electrostatic interactions between the two negatively charged groups and/or steric strain. The introduction of the aspartic acid in the absence of glutamic acid at position 60 (T58DE60A mutant) will not result in such unfavorable interactions. In this case, the interaction energy is a measure of the unfavorable interactions between Asp-58 and Glu-60.

Contribution of Residues in the Reactive Site Loop to Protein Activity. The presence of both Thr-58 and Glu-60 make significant contributions to the inhibitory activity of the protein: there is a significant increase in K_i, 80 and 140 fold on mutation of T58A and E60A, respectively, representing decreases in binding energy of 2.6 and 2.9 kcal mol^{-1}, respectively. Thr-58 and Glu-60 make no contacts with subtilisin BPN′ in the crystal structure of the subtilisin BPN′:chymotrypsin inhibitor 2 complex (McPhalen et al., 1985). The effects of these mutations on the stability of the complex must, therefore, be due to intramolecular and not intermolecular interactions.

Although mutation of T58D has little or no effect on the stability of the protein (Table 2), it is found to have a large effect on the inhibitory activity of the protein and destabilizes the subtilisin BPN′:CI2 complex by 2 kcal mol^{-1}. The side chain in the free inhibitor is exposed to solvent. In this case, it is possible that the larger aspartic acid group introduces little, or no, steric strain. In the complex, however, the side chain is buried in a densely packed region, and the larger aspartic acid group may be more difficult to accommodate without some unfavorable steric strain.

All mutations are found to have a much larger effect on the stability of the complex than on the stability of the free inhibitor. This may result from the difference in the environment of the residues in the free inhibitor and in the complex. In the former, the side chains are largely exposed to solvent. This has two effects. First, the effective dielectric constant may be close to that for water. In comparison, the side chains in the complex are completely buried and the effective dielectric constant will be significantly lower. In this case, electrostatic interactions will be larger. It has been shown that the strength of hydrogen bonds and salt bridges varies according to environment. Whereas hydrogen bonds and salt bridges on the surface of proteins are found to have only a small effect on stability, buried hydrogen bonds and salt bridges are found to have a much larger effect. A buried charge without a partner, for example, will result in a major destabilizing effect on protein stability (3−4 kcal mol^{-1}; Fersht, 1972, 1987, 1988). In principle, the net contribution of a hydrogen bond between two groups in a protein will be small, since it will reflect only the difference between the energies of interaction of the groups with each other relative

to the interaction of those hydrogen-bonding groups with water (Fersht, 1985). The burial of a charged hydrogen bond donor or acceptor without its partner will, however, be very destabilizing. In addition, the side chains in the complex are in a more densely packed environment than in the free inhibitor. Thus, unfavorable steric interactions in the complex will be worse.

Interaction between Thr-58/Asp-58 and Glu-60 in Complex with Subtilisin BPN'. The interaction energy between a threonine or aspartic acid group at position 58 and the glutamic acid group at position 60 in the complex between subtilisin BPN' and CI2 has been calculated using double mutant cycles. The interaction energies are 2.10 ± 0.13 and 4.23 ± 0.16 kcal mol^{-1} measured for T58AE60A and T58DE60A, respectively. Thus, there is a significant interaction between these residues in the complex. These interaction energies are significantly larger than those measured in the free inhibitor. For T58AE60A, the interaction energy is a measure of the strength of the hydrogen bond between the hydroxyl of Thr-58 and the $O^{\epsilon 2}$ of Glu-60. The hydrogen bond is much weaker in the free inhibitor where the dielectric constant is high and there is access of water to the site of mutation. For T58DE60A, the interaction energy has contributions from unfavorable electrostatic interactions and steric strain. Both of these factors will be more important in the complex than in the free inhibitor because the side chains are buried and there is a low effective dielectric constant, no access of water to the site of mutation, and close-packing of the side chains.

Mechanism of Inhibition of Subtilisin BPN' by Chymotrypsin Inhibitor 2. Previous kinetic studies on CI2 (Longstaff et al., 1990) have found that the kinetic data are consistent with a simple bimolecular association, where inhibitor binds with minimal change in inhibitor structure such that the EI adduct represents a frozen Michaelis complex or something closely related to it. The data presented here are also consistent with this mechanism; i.e., plots of $(v_o - v_s)/v_s$ are linear over the inhibitor concentration range studied. It has been proposed that hydrolysis of the scissile bond is slow in wild-type CI2 because (i) inhibitor binds tightly to the enzyme leading to a very stable complex and (ii) the activation barrier for hydrolysis is raised by having an inflexible peptide in the substrate binding cleft. In this way the EI complex is in a thermodynamic "pit" with a large barrier preventing hydrolysis (Longstaff et al., 1990). Data presented here support this hypothesis. Mutants of CI2 that significantly decrease the binding energy and decrease the stability/flexibility of the reactive site loop also show temporary inhibition due to the slow hydrolysis of the scissile bond.

Comparison of the data for T58A and E60A in the free inhibitor and in the complex shows that, whereas the destabilization energies for the two mutants are very similar in the free inhibitor, E60A is significantly more destabilizing in the complex. This suggests that the interactions made by Glu-60 are more critical for inhibition than those made by Thr-58. The $O^{\epsilon 2}$ of Glu-60 makes a hydrogen bond with its own amide proton. Previous studies on eglin c have shown that this hydrogen bond is important for inhibition (Bode et al., 1986; Heinz et al., 1992). Our studies agree with this conclusion. In addition, the double mutant T58DE60A has little effect on the stability of the complex. We propose that this could, in part, be due to the aspartic acid replacing the interactions made by Glu-60, including the hydrogen bond to the backbone amide of residue 60.

Hydrolysis of Destabilized CI2 Mutants by Subtilisin BPN'. By comparison of data from destabilizing mutants in the active site loop and in the hydrophobic core of CI2, we have shown that the hydrolysis of CI2 does not result from the global destabilization of the protein but must be a consequence of local destabilization of the reactive site loop. The reversal of inhibition due to the hydrolysis of the inhibitor can be limited by either the rate of hydrolysis of the scissile bond, i.e., the equilibrium constant between cleaved (EI*) and noncleaved (EI) forms of the bound inhibitor, or by dissociation of the EI* complex. For T58AE60A, $k_d = 3.5 \times 10^{-4}$ s^{-1}. This value is close to the values of k_{off} determined for the more destabilized mutants; see Table 3. This suggests that the rate-limiting step is the dissociation of the EI* complex. It is perhaps interesting to note that, with the exception of T58D, there is a very strong correlation between the destabilization energy in the free inhibitor and in the complex (the slope of the plot is 4.3, the intercept is −0.3, and the correlation coefficient is 0.99).

CONCLUSIONS

Thr-58 and Glu-60, residues whose functional groups are conserved among the potato inhibitor I family of serine protease inhibitors, have some importance in the stability of the free inhibitor. They are far more important, however, for the stability of enzyme−inhibitor complex and are essential for the activity of CI2. These residues take part in the hydrogen-bonding and salt bridge network within the active site loop which is a characteristic of this family of inhibitors.

REFERENCES

Akke, M., & Forsén, S. (1990) *Proteins: Struct., Funct., Genet. 8*, 23−29.

Alber, A. (1989) *Annu. Rev. Biochem. 58*, 765−798.

Alber, T., Dao-Pin, S., Wilson, K., Wozniak, J. A., Cook, S. P., & Matthews, B. W. (1987) *Nature 330*, 41−46.

Bode, W., Papamokos, E., Musil, D., Seemuller, U., & Fritz, H. (1986) *EMBO J. 5*, 813−818.

Boisen, S., Andersen, C. Y., & Hejgaard, J. (1981) *Physiol. Plant 52*, 167−176.

Cha, S. (1975) *Biochem. Pharmacol. 24*, 2177−2185.

Dao-Pin, S., Nicholson, H., & Matthews, B. W. (1991) *Biochemistry 30*, 7142−7153.

Fersht, A. R. (1972) *J. Mol. Biol. 64*, 497−509.

Fersht, A. R. (1985) *Enzyme Structure and Mechanism*, W. H. Freeman and Company, New York.

Fersht, A. R. (1987) *Trends Biochem. Sci. 12*, 301−304.

Fersht, A. R. (1988) *Biochemistry 27*, 1577−1580.

Fersht, A. R., Shi, J.-P., Knill-Jones, J., Lowe, D. M., Wilkinson, A. J., Blow, D. M., Brick, P., Carter, P., Waye, M. M. Y., & Winter, G. (1985) *Nature 314*, 235−238.

Goldstein, A. (1944) *J. Gen. Physiol. 27*, 529.

Heinz, D. W., Hyberts, S. G., Peng, J. W., Priestle, J. P.,Wagner, G., & Grutter, M. G. (1992) *Biochemistry 31*, 8755−8766.

Horovitz, A., & Fersht, A. R. (1990) *J. Mol. Biol. 214*, 613−617.

Horovitz, A., Serrano, L., Avron, B., Bycroft, M., & Fersht, A. R. (1990) *J. Mol. Biol. 216*, 1031−1044.

Jackson, S. E., & Fersht, A. R. (1991a) *Biochemistry 30*, 10428−10435.

Jackson, S. E., & Fersht, A. R. (1991b) *Biochemistry 30*, 10436−10443.

Jackson, S. E., & Fersht, A. R. (1993) *Biochemistry 32*, 13909–13916.
Jackson, S. E., Moracci, M., elMasry, N., Johnson, C. M., & Fersht, A. R. (1993a) *Biochemistry 32*, 11259–11269.
Jackson, S. E., elMasry, N., & Fersht, A. R. (1993b) *Biochemistry 32*, 11270–11278.
Jonassen, I. (1980) *Carlsberg Res. Commun. 45*, 47–48.
Kraulis, P. (1991) *J. Appl. Crystallogr. 24*, 946–950.
Laskowski, M., &. Kato, I. (1980) *Annu. Rev. Biochem. 49*, 593–626.
Longstaff, C., Campbell, A. F., & Fersht, A. R. (1990) *Biochemistry 29*, 7339–7347.
Ludvigsen, S., Shen, H. Y., Kjaer, M., Madsen, J. C., & Poulsen, F. M. (1991) *J. Mol. Biol. 222*, 621–635.
McPhalen, C. A., & James, M. N. G. (1987) *Biochemistry 26*, 261–269.
McPhalen, C. A., Svendsen, I., Jonassen, I., & James, M. N. G. (1985) *Proc. Natl. Acad. Sci. U.S.A. 82*, 7242–7246.
Neurath, H. (1984) *Science 224*, 350–357.
Sali, D., Bycroft, M., & Fersht, A. R. (1991) *J. Mol. Biol. 220*, 779–788.
Sander, C., & Schneider, R. (1991) *Proteins: Struct., Funct., Genet. 9*, 56–68.
Sayers, J. R., Schmidt, W., & Eckstein, F. (1988) *Nucleic Acids Res. 16*, 791–802.
Serrano, L., Kellis, J. T., Cann, P., Matouschek, A., & Fersht, A. R. (1992) *J. Mol. Biol. 224*, 783–804.
Wagner, G., Hyberts, S. G., Heinz, D. W., & Grutter, M. G. (1990) *Structure & Methods Vol. 2, DNA Protein Complexes & Proteins*, Adenine Press, Albany, NY.
Williams, J. W., & Morrison, J. F. (1979) *Methods Enzymol. 63*, 437–467.